PIBB 生物化学与生物物理进展
Progress in Biochemistry and Biophysics
2024, 51(5): 1174~1190
www.pibb.ac.cn

Shakuyakukanzoto Relieves Ulcerative Colitis in Mice by Regulating The Expression of NDUFS1 and Inhibiting The Polarization of Macrophages to M1

XIAHOU Zhi-Kai[1)], XIAO Hong[2)], SONG Ya-Feng[1)*], HAN Jun[3)*]

([1)]*China Institute of Sport and Health Science, Beijing Sport University, Beijing* 100084, China;
[2)]*Department of Sport and Science, Beijing Sport University, Beijing* 100084, China;
[3)]*Chinese Medicine Research Institute of Beijing Tcmages Pharmaceutical Co., Ltd., Beijing* 101301, China)

Graphical abstract

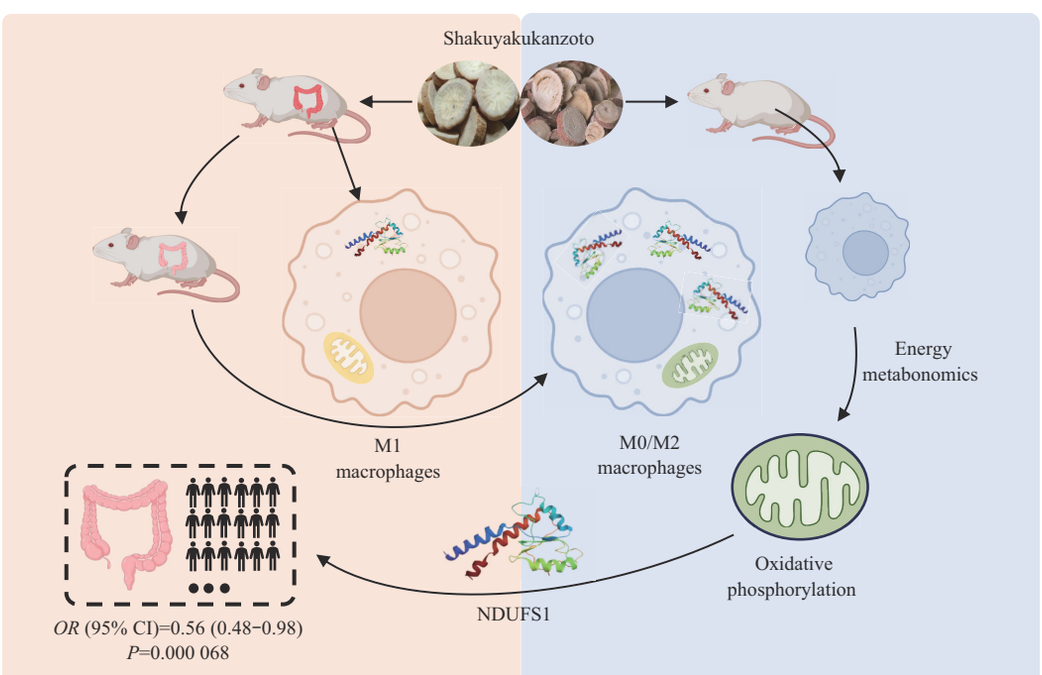

Abstract **Objective** This study aims to explore and elucidate the possible mechanism of action of Shakuyakukanzoto (SKT) in improving ulcerative colitis (UC) in mice through regulating energy metabolism and polarization of macrophages. **Methods** The mouse UC model was constructed by administering 3% dextran sulfate sodium salt (DSS), and the mice were treated with SKT intragastrically. In addition, single-cell sequencing and enrichment of metabolic pathways against two datasets, GSE21157 and

* Corresponding author.
SONG Ya-Feng. Tel: 86-10-62962180, E-mail: songyafeng@bsu.edu.cn
HAN Jun. Tel: 86-18311059115, E-mail: 729229056@qq.com
Received: September 2, 2023 Accepted: October 26, 2023

GSE210415, were conducted first. Second, the extraction and metabolomics of peritoneal macrophages from UC mice were verified. Then, the pathway of differentially abundant metabolite enrichment and the correlation of UC risk were analyzed depending on univariate Mendelian randomization of two samples weighted by standard inverse variance. Finally, the results were verified by qRT-PCR, Western blot, and flow cytometry. **Results** According to the HE staining results, SKT can significantly alleviate colon damage caused by DSS. Macrophages, NK cells, T cells, and more than 10 different types of cells, based on single-cell sequencing analysis, are detected in the intestinal wall. In the disease group, we can conclude that the activity of 49 macrophage metabolic pathways, mainly involved in energy metabolism, is significantly upregulated through a comparison of the two datasets. In energy metabolomics, 10 and 18 types of metabolites accompanied by significantly upregulated and downregulated differential expression were identified in the treatment group and the model group, as well as the model group and the blank group, respectively. Meanwhile, these differentially expressed metabolites present an obvious correlation with glycolysis and oxidative phosphorylation. Moreover, it can be inferred that glycolysis and the oxidative phosphorylation-related gene *NDUFS1* (*OR*: 0.56, 95% CI: 0.48−0.98, *P*=0.000 068) are associated with a reduced risk of UC based on the univariate Mendelian randomization of two samples weighted based on standard inverse variance. By analyzing the difference in transcription levels between the two datasets, the transcription level of NDUFS1 in UC was decreased compared with that in the normal group. The results of qRT-PCR, Western blot, and flow cytometry indicate that SKT can promote the expression of the oxidative phosphorylation protein NDUFS1 in macrophages and inhibit the M1-type polarization of macrophages. Furthermore, knockdown/overexpression of NDUFS1 can affect the effect of SKT on M1-type polarization of macrophages. **Conclusion** Based on the results of this study, SKT inhibits macrophage polarization toward the M1 phenotype by regulating the level of the oxidatively phosphorylated protein NDUFS1 in macrophages; hence, UC is also relieved in mice. These conclusions not only reveal the therapeutic mechanism of SKT for UC but also provide a new theoretical basis for clinical application.

Key words Shakuyakukanzoto, macrophage polarization to M1, oxidative phosphorylation, ulcerative colitis
DOI：10.16476/j.pibb.2023.0347

As a type of chronic and recurrent disease, ulcerative colitis (UC) mainly affects the internal colonic layer and causes diarrhea, abdominal pain, and other digestive complications. Despite the considerable progress achieved in modern medicine, the pathogenesis of UC remains unclear and is generally considered to be correlated with heredity, environmental factors, abnormal immune responses, and intestinal flora imbalance[1]. Many inflammatory cells infiltrate pathological mucosal tissues, which is one of the characteristics of UC. Macrophages, which serve as the first line of defense for the innate immune system, play a key role in the progression of UC[2]. Macrophages can be polarized into two states: M1 macrophages and M2 macrophages[3]. After being activated, M1 macrophages can secrete a variety of inflammatory mediators, thus aggravating the inflammatory response. However, M2 macrophages exert their effect in the later stage of the inflammatory response and promote tissue repair. Therefore, an important strategy for UC treatment lies in regulating the balance between these two types of macrophages.

Shakuyakukanzoto (SKT), which originated from *Treatise on Febrile Diseases*, was also the first batch of ancient classical prescriptions published by the National Administration of Traditional Chinese Medicine, and it has been used to treat many diseases in East Asia, especially in Japan. The main components of SKT include *Glycyrrhiza uralensis* Fisch. and *Paeonia lactiflora*, both of which have rich pharmacological activities. *Paeonia lactiflora* is considered to have anti-inflammatory, immunomodulatory, and anticoagulant effects[4], while it is deemed that *Glycyrrhiza uralensis* Fisch. has spasmolytic and liver-protecting effects[5]. In addition, some studies have shown that SKT can relieve UC induced by dextran sulfate sodium (DSS) by downregulating ferroptosis[6]. From the clinical point of view, SKT and its modified formulas have good therapeutic effects on UC with various patterns of syndromes[7]. With increasing attention to Chinese herbal medicine and traditional medicine in recent years, researchers have begun to study the application of these traditional preparations in modern medicine. SKT has aroused much attention by virtue of its unique combination of pharmaceutical effects and high safety. An in-depth pharmacodynamics and pharmacokinetics study on SKT has shown that no

obvious change is observed in the behavior of normal animals after administration at a dose of 1 g/kg, without significant drug intervention effects on the main physiological indices of the central nervous system, the respiratory system, the cardiovascular system, the gastrointestinal system, and the renal system[8]. In addition, many clinical trials have shown that SKT is widely used to relieve symptoms such as acute muscle spasm, muscle-joint pain, stomachache, and abdominal pain[9]. In the field of molecular pharmacology, the anti-inflammatory, antioxidant, and neuroprotective effects manifested in SKT may be related to some key biomarkers and the regulation of cell signaling pathways, which play a core role in inflammation and the oxidative stress response[10-12].

However, little is known about how SKT affects UC, especially the specific mechanism of action in UC. Considering the complex pathophysiological mechanism of UC and its close relationship with immune cells, studying the mechanism of SKT in UC can not only provide new therapeutic strategies for UC patients but also help to deeply understand the pathophysiological basis of UC. This study aims to systematically explore the therapeutic effect of SKT on UC and its potential mechanism in relieving UC by regulating the polarization state of macrophages. The flowchart is shown in Figure 1. This study is expected to provide a new idea for UC treatment and lay a solid foundation for future clinical applications.

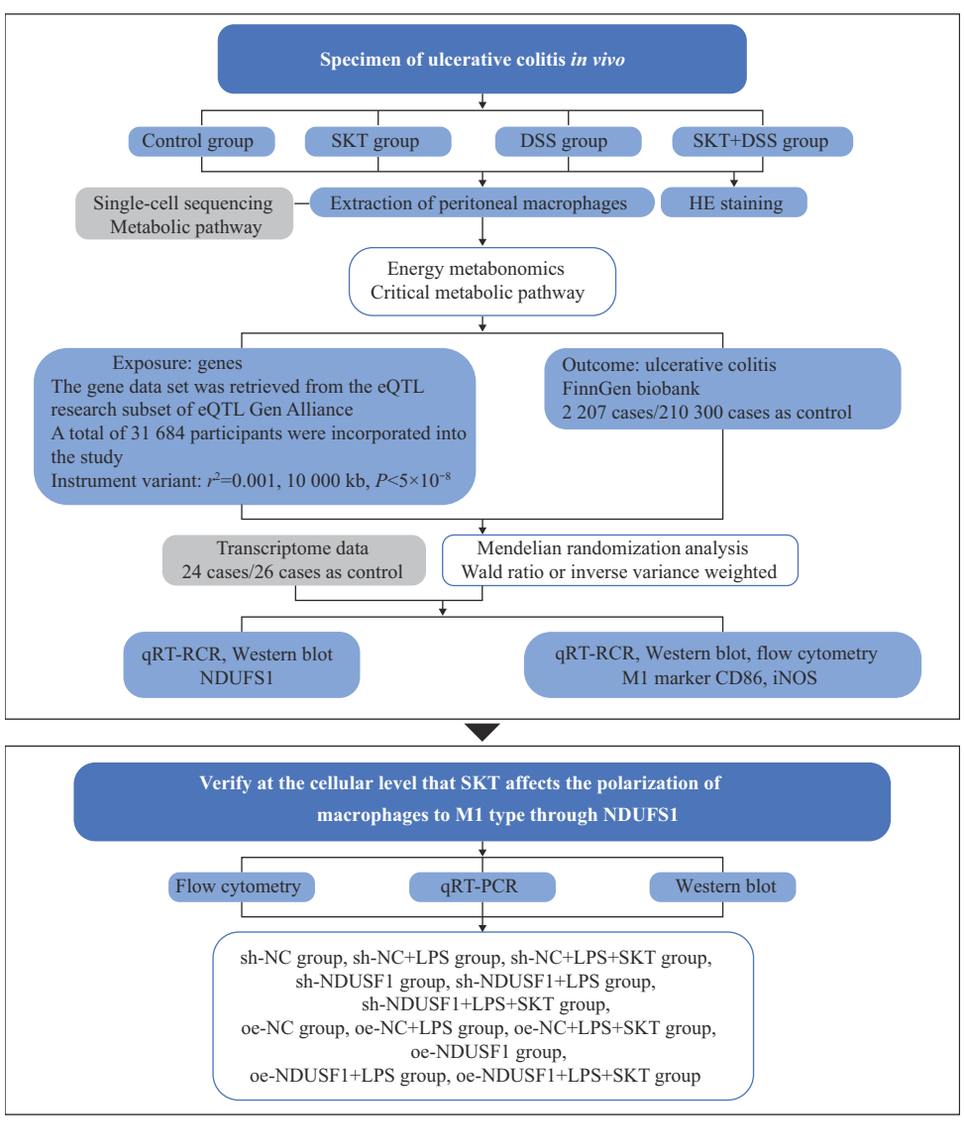

Fig. 1 Experimental design flowchart of Shakuyakukanzoto for alleviating ulcerative colitis in mice

1 Materials and methods

1.1 Experimental materials

C57BL/6 mice were purchased from Nanjing GemPharmatech Co., Ltd.; the mouse macrophage line RAW264.7 from ATCC cell bank; lipopolysaccharide (LPS) from Sigma; DMEM and fetal bovine serum (FBS) from HyClone company; cell culture plates from Corning company; dextran sodium sulfate (DSS) from Yeasen company; *Paeonia lactiflora* and *Glycyrrhiza uralensis* Fisch. from Chinese prescriptions in Tsumura, Japan; high-performance liquid chromatography acetonitrile and methanol from Merck; Milli-Q water used in all experiments from Millipore company; all standard samples from Sigma-Aldrich; and formic acid from Sigma-Aldrich. Standard stock solutions with a concentration of 1 g/L were prepared in methanol and other solutions. All stock solutions were stored at −20℃ . Before analysis, the stock solutions were diluted with methanol into working solutions.

1.2 Animal modeling and drug administration

C57BL/6 mice were divided into 4 groups: control group, SKT group, DSS group, and SKT+DSS group, with 6 mice in each group. In the control group and SKT group, mice were given normal drinking water; in the DSS group and SKT+DSS group, mice were given drinking water containing 3% DSS for 7 d to induce acute colitis; in the SKT group and SKT+DSS group, mice were treated with 1 g/kg SKT by intragastric administration once a day, and the administration was started one week before the start of modeling for 14 consecutive days. The weight changes and disease activity index (DAI) scores of the mice in each group were recorded every day after the start of modeling. All procedures were carried out in accordance with the guidelines and approval of the Ethics Committee of Beijing Sport University. Approved by the Ethical Review Committee of Animal Experiments of Beijing Sport University (approval No.: 2023028A), all experiments met the ARRIVE criteria. The experimental animal quality certificate number was 202211254, the experimental animal production license number was NO. SCXK (Su) 2018-0008, and the occupancy permit number of feeding facilities was NO. SYXK (Su) 2018-0012.

1.3 Detection of colonic pathological injury through HE staining

Colon tissue samples with a length, width, and height of 0.5 cm were taken, fixed in room-temperature buffer containing 4% paraformaldehyde, and then embedded in paraffin. Slices 5 μm in thickness were prepared, dyed with hematoxylin aqueous solution for 3 min, dehydrated in 70% and 90% alcohol for 10 min, dyed with eosin for 3 min, dehydrated again, and finally hyalinized using xylene. Histopathological features were observed under an optical microscope. The scoring standards for colonic pathology are listed in Table 1.

Table 1 Scoring criteria of colon pathology

Score	Inflammation condition	Depth of the lesion	Destruction of the crypt	Extent of the lesion/%
0	None	None	None	None
1	Mild	Submucosa	1/3 of the crypt of the basement membrane was destroyed	1−25
2	Severe	Muscular layer	2/3 of the crypt of the basement membrane was destroyed	26−50
3	—	Serosa layer	Only the superficial epithelium was intact	51−75
4	—	—	All crypts and epithelium were destroyed	76−100

Five different fields of vision of HE-stained sections were randomly observed, and pathological scores were given.

1.4 Extraction of peritoneal macrophages

Five milliliters of precooled PBS solution were intraperitoneally injected into mice immediately after sacrifice, and the injection site was then massaged for 5 min to facilitate intensive mixing. Subsequently, the exodermis of mice was cut open, and as much as possible of the peritoneal PBS solution was removed using a syringe needle for centrifugation at 30*g* for 5 min. The supernatant was discarded, the cell precipitates were resuspended using PBS, centrifugation at 300*g* was performed for 5 min again, and then the supernatant was discarded. Next, the precipitates were added to DMEM culture medium containing 10% FBS and inoculated into a 12-well plate (2×10^5 cells were added to each well). After culturing in a cell culture box for 2 h, the culture plate was gently rinsed twice using PBS, and the peritoneal macrophages attached to the culture plate were

collected using a cell scraper. Afterward, the collected cell precipitates were resuspended in PBS for treatment before metabonomic sequencing.

1.5 Single−cell sequencing analysis

Two single-cell sequencing datasets (GSE211578 and GSE210415) were downloaded from the GEO database. The cells with fewer than 15% mitochondrial genes were adopted forsubsequent analysis. First, the sequencing data were subjected to principal component analysis (PCA) dimension reduction analysis *via* the Seurat software package, and each cell was clustered through the UMAP method. To further clarify the cell type, each cell subpopulation was annotated using the SingleR software package. To acquire the activity of each metabolic pathway in macrophages, a gene set containing 113 metabolic pathways was downloaded from the GSEA website, and each metabolic pathway was scored using the GSVA software package. The Limma data package was used to calculate the intergroup difference in metabolic pathways.

1.6 Energy metabolomics

The sample was thawed on ice, mixed with 500 μl of 80% methanol/water (precooled to 20° C), and vortexed at 2 500 r/min for 2 min. Next, the sample was frozen in liquid nitrogen for 5 min, thawed on ice for 5 min, and vortexed for 2 min, followed by centrifugation at 12 000 r/min below 4°C for 10 min. Then, 300 μl of supernatant was taken, put into a new centrifuge tube, and placed in a −20° C refrigerator for 30 min. After centrifugation, 200 μl of supernatant was taken and put on a protein precipitation plate for further LC-MS analysis.

The flowing-phase ultrapure water (10 mmol/L ammonium acetate, 0.3% ammonia water) was phase A, and 90% acetonitrile/water (*v*/*v*) was phase B, which were subjected to gradient elution (0−1.2 min, 5%A; 1.2−8 min, 5%A−30%A; 8−9 min, 30%A−50%A; 9−11 min, 50%A; 11.1−15 min, 50%A−5%A). The flow rate was 0.40 ml/min, the column temperature was 40° C, and the injection volume was 2 μl. The electrospray ionization (ESI) temperature was 550° C, the mass spectral voltage was 5 500 V in positive ion mode and −4 500 V in negative ion mode, and the curtain gas (CUR) was 35 psi. In QTRAP 6500+ , each ion pair was scanned and detected according to the optimized declustering potential (DP) and collision energy (CE).

All these metabolites were detected by MetWare (http://www.metware.cn/) based on the AB Sciex QTRAP 6500 LC-MS/MS platform. Mass spectral data were processed using MultiQuant 3.0.3 software. By reference to the retention time and peak pattern information of standard samples, the chromatographic peaks of the detection object detected from different samples were subjected to integral correction to ensure accurate qualification and quantification. Then, PCA and orthogonal partial least squares-discriminant analysis (OPLS-DA) were performed, and the chemical compounds whose projection value of variable importance satisfied (*VIP*) ⩾1 with $P<0.05$ were screened out as potential biomarkers, followed by metabolic pathway enrichment analysis of such biomarkers on this website.

1.7 Mendelian randomization analysis

The causal relationships of all cis-regions and some trans-regions expressed by whole blood genes with UC were explored through single-variable MR (SVMR) and reverse Mendelian randomization (MR) methods. In SVMR, the estimated value was acquired using different methods, including inverse-variance weighted (IVW), MR-Egger, weighted median (WM), and weighted mode. Single tools were subjected to the Wald ratio test: the estimated Wald value was solved by dividing the single nucleotide polymorphism (SNP) result by the SNP exposure factor. Only if SNPs were mutually independent and target pleiotropy was not observed was the result obtained by the IVW method considered most reliable. The above analysis was implemented *via* R 3.6.3 software and the R software package TwoSampleMR.

According to the summary statistics, several genetic variations were used as independent variables in MR research. The SNPs of gene expression genetics came from the eQTL research subset of eQTLGen Alliance, which involved 31 684 European participants. The genome-wide association studies （GWAS) statistical summary was derived from the 5th round of analysis of the Finnish Gene Biobank, including 212 507 participants (2 207 cases and 210 300 controls). All GWAS summary datasets were publicly available fromhttps://gwas. mrcieu. ac. uk/datasets/.

In univariate MR analysis, the causal relationship between gene expression and UC was evaluated first. When choosing the independent variables, all the gene

variations significantly correlated with gene expression ($P<5\times10^{-8}$) were taken into account. Considering the linkage disequilibrium between SNPs, the datasets were coordinated by eliminating SNP(c) with potential linkage disequilibrium. Then, the SNPs significantly related to the results ($P<5\times10^{-8}$) were excluded. Finally, the SNPs meeting the standard were included in the two-way MR analysis.

1.8 Transcriptomic data analysis

With "Ulcerative Colitis" as the keyword, the gene expression profile was searched based on the GEO database (http://www.ncbi.nlm.nih.gov/geo), and the human samples of "*Homo sapiens*" were selected to obtain datasets numbered GSE128682 and GSE102746. The platform number of the GSE128682 dataset was GPL21697, which included 16 normal colon samples and 14 UC samples. The platform number of the GSE102746 dataset was GPL16791, which contained 10 normal colon samples and 10 UC samples.

The datasets of NADH: ubiquinone oxidoreductase core subunit S1 (NDUFS1), hexokinase (HK), recombinant cytochrome C oxidase subunit IV isoform 1 (COX4I1), and triosephosphate Isomerase (TPI) in GSE128682 and GSE102746 were extracted, their quantitative expression values in the normal colon group and UC group were standardized based on the conversion of $\log_2$, and subsequently, their expression differences in normal colon tissues and UC tissues were analyzed through double-sample *t* tests.

1.9 Transfection, administration, and grouping of macrophages

RAW264.7 cells were cultured using DMEM culture medium containing 10% FBS, and the experiment was carried out when the cell density reached 70%−80%. Then, 3×10^5 RAW264.7 cells were inoculated into a 6-well plate, and lentivirus was used to knock down NDUFS1 (sh-NDUFS1), knock down NC (sh-NC), overexpress NDUFS1 (oe-NDUFS1), and overexpress NC (oe-NC). Forty-eight hours later, the cells were screened using puromycin to acquire RAW264.7 cells with NDUFS1 knockdown and NDUFS1 overexpression, which were grouped as follows: the sh-NC group, sh-NC+LPS group, sh-NC+LPS+SKT group, sh-NDUFS1 group, sh-NDUFS1+LPS group, sh-NDUFS1+LPS+SKT group, oe-NC group, oe-NC+LPS group, oe-NC+LPS+SKT group, oe-NDUFS1 group, oe-NDUFS1+LPS group, and oe-NDUFS1+LPS+SKT group. In the sh-NC+LPS+SKT group, sh-NDUFS1+LPS+SKT group, oe-NC+LPS+SKT group and oe-NDUFS1+LPS+SKT group, 100 μg/L SKT was added for coincubation for 12 h; in the sh-NC+LPS group, sh-NC+LPS+SKT group, sh-NDUFS1+LPS group, sh-NDUFS1+LPS+SKT group, oe-NC+LPS group, oe-NC+LPS+SKT group, oe-NDUFS1+LPS group, and oe-NDUFS1+LPS+SKT group, 100 μg/L LPS was added for coincubation for 12 h. The sh-NDUFS sequence was AAGAATGGATCTCTGATAAAACCAG, and the sh-NC sequence was GCAACAAGATGAAGAGCACCAA.

1.10 Detection of inducible nitric oxide synthases (iNOS) and NDUFS1 mRNA expression based on qRT−PCR

The total RNA of cells in each group was extracted using TRIzol reagent and reverse transcribed into cDNA in accordance with the instructions of the reverse transcription kit. The corresponding systems were prepared according to the instructions of the qPCR kit, and each group was detected in triplicate. Next, qPCR was conducted using a TB GreenTM Premix Ex Taq II kit under the following conditions: 95° C for 30 s (1 cycle), 95° C for 5 s, and 60° C for 30 s (40 cycles), and data analysis was performed through the $2^{-\Delta\Delta Ct}$ method. The experiment was repeated separately 3 times as follows: NDUFS1-qF: 5'-GCTGTTTCTTCTGGGAGCAG-3', NDUFS1-qR: 5'-TAACATCAGCCATGGGAGCA-3'; iNOS-qF: 5'-TTTGTGCGAAGTGTCAGTGG-3', iNOS-qR: 5'-CCTCCTTTGAGCCCTTTGTG-3'; GAPDH-qF: 5'-CAGAACATCATCCCTGCATC-3', and GAPDH-qR: 5'-TACTTGGCAGGTTTCTCCAG-3'.

1.11 Western blot analysis of iNOS and NDUFS1 protein expression

Macrophages in each group were collected, and RIPA lysate containing protease inhibitor was added and lysed on ice for 30 min. After that, centrifugation was carried out at 13 000 r/min and 4° C for 15 min, and the supernatant was transferred to a new centrifuge tube and then measured by the BCA method. Ten micrograms of total protein was loaded through SDS-PAGE and transferred to a PVDF membrane. Subsequently, the PVDF membrane was placed in 5% skim milk powder and sealed at room temperature for 1 h. Then, diluted iNOS, NDUFS1,

and HK1 primary antibodies were added and incubated overnight on a shaker at 4°C. The membrane was washed with PBST three times (for 10 min each time), the HRP-labeled secondary antibody corresponding to the species of the primary antibody was added and incubated on a shaking table at room temperature for 1 h, and the membrane was washed with PBST three times (for 10 min each time). Color development and luminescence were performed using ECL chemiluminescence liquid, followed by photographing with a gel-imaging system and protein band analysis with the Image-Pro Plus image analysis system.

1.12 Detection of the proportion of CD86− and CD206−positive cells *via* flow cytometry (FCM)

The peritoneal macrophages and RAW264.7 cells in each group were collected, washed twice with PBS solution containing 5% FBS, incubated with primary antibodies against CD86 and CD206, and incubated at 4° C for 1 h. Then, PBS solution was added for rinsing twice, and centrifugation was performed at 1 000 r/min and 4° C for 5 min. Then, 200 μl of PBS was added for resuspension, and detection was performed through a flow cytometer. M1- or M2-positive cell ratio= (CD86+ cells or CD206+ cells)/total cells×100%.

1.13 Statistical analysis

In this study, statistical analysis was conducted *via* GraphPad Prism 6.0 software, and all data are expressed as the mean±standard deviation. Moreover, all data were independently analyzed at least 3 times. $P<0.05$ indicated statistical significance.

2 Results

2.1 SKT relieves DSS−induced UC symptoms

The daily weight monitoring results showed that there was no obvious change in the weight of mice in the control group and SKT group, indicating no biotoxicity of SKT at this concentration. The body weight of mice in the DSS group decreased gradually with the modeling. Compared with the DSS group, the weight loss declining trend of mice in the SKT+DSS group slowed down, as shown in Figure 2a. The daily DAI monitoring results revealed that there was no DAI score for mice in the control group and SKT group, and the DAI scores of DSS group mice increased gradually with the modeling. Compared with the DSS group, the increasing trend in the DAI of mice in the SKT+DSS group slowed, as shown in Figure 2b.

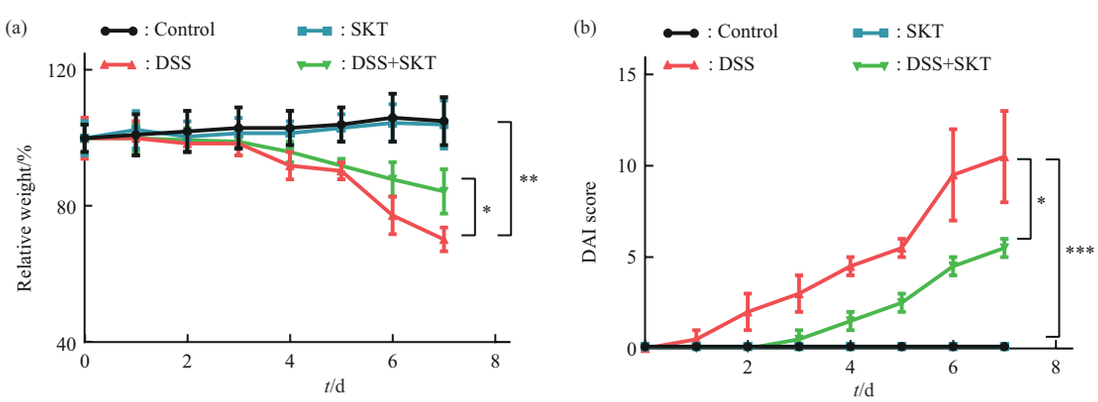

Fig. 2 Comparison of weight changes and disease activity index (DAI) scores of mice in each group

Male C57BL/6 mice were randomly divided into a control group, model group, and treatment group. Mice in the control group were given normal drinking water, those in the model group were given drinking water containing 3% DSS for 7 d to induce acute colitis, and those in the treatment group were given drinking water containing 3% DSS for 7 d to induce acute colitis and treated through intragastric administration at a dose of 1 g/kg once per day, which was started one week before modeling and implemented for 14 consecutive days. Since modeling, the weight change (a) and disease activity index (DAI) scores (b) of mice in each group were recorded every day. The data are expressed as the mean±standard deviation (n=3). *P<0.05, **P<0.01, ***P<0.001.

2.2 SKT relieves colonic pathological injury

The colonic pathological results showed that the colon structure of mice in the control group and SKT group was intact, accompanied by clear villus and crypt structures and serious colon injuries, indicating that DSS-induced acute colitis modeling succeeded. In the SKT+DSS group, the colon structure of mice partially recovered, and crypt and villus structures

could be observed, revealing that SKT had the function of preventing DSS-induced UC, as shown in Figure 3.

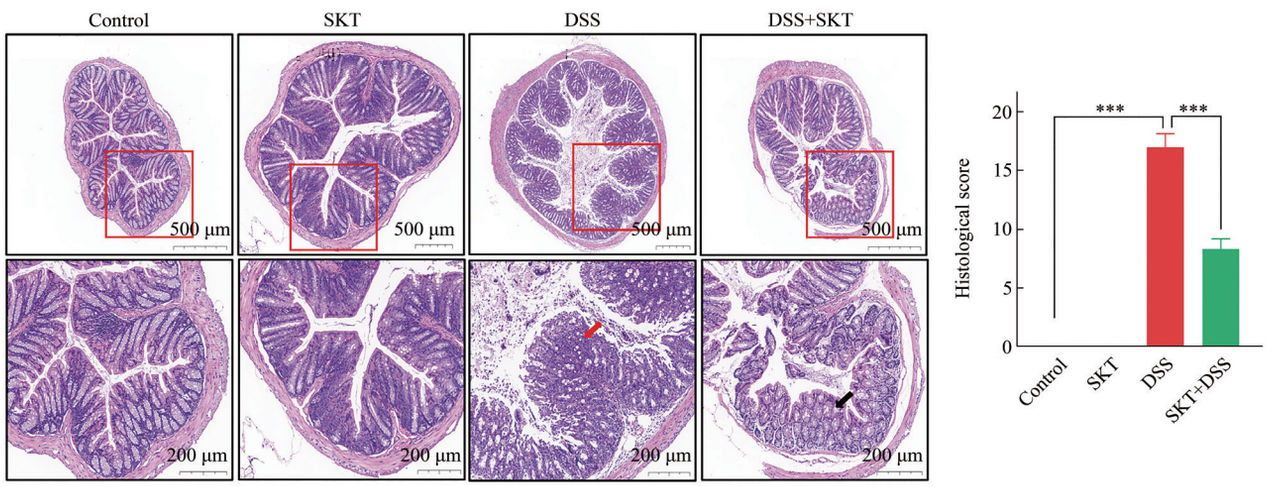

Fig. 3　Comparison of pathological colonic damage in mice in each group

Male C57BL/6 mice were randomly divided into control group, model group, and treatment group. Mice in the control group were given normal drinking water, those in the model group were given drinking water containing 3% DSS for 7 d to induce acute colitis in mice, and those in the treatment group were given drinking water containing 3% DSS for 7 d to induce acute colitis and treated through intragastric administration at a dose of 1 g/kg once per day, which was started one week before modeling and implemented for 14 consecutive days. Colon tissue samples from mice were collected and subjected to HE staining to evaluate pathological colonic damage in mice in each group. The red arrow shows that the mucosal layer of the colon of mice in the model group was completely damaged, and the villi and crypt structures disappeared completely; the black arrow shows that the mucosal layer of the colon of the mice in the treatment group was restored, and obvious villi and crypt structures could be seen. ***P<0.001.

2.3　Distribution of macrophagic metabolic pathways by single−cell sequencing in UC

Figure 4a shows the distribution of each cell type in the two datasets. Through single-cell sequencing, more than 10 kinds of cells were found in the intestinal wall, such as adipocytes, B cells, dendritic cells, endothelial cells, epidermal cells, granulocytes, macrophages, monocytes, neurons, NK cells, and T cells. Meanwhile, evident heterogeneity in the composition of cell types was also found between the disease group and the normal group. Figure 4b displays the distribution of macrophages in the two datasets. In this study, it was discovered that macrophages could be further divided into 10 clusters, and there was apparent heterogeneity between the disease group and the normal group in the composition of macrophage clusters. Figure 4c shows the distribution of different macrophagic metabolic pathways in the two datasets. The activity of a total of 49 metabolic pathways in the disease group was significantly upregulated in the two datasets, and the activity of only one metabolic pathway was apparently downregulated. Figure 4d gives the changes in cross difference pathways between the two datasets.

2.4　Macrophagic metabolic pathway enrichment results based on energy metabolomics

The PCA results of the data are described in Figure 5a, b. The data points in the blank group and model group were obviously separated, indicating evident metabolic differences between the 2 groups. After drug administration, the data points in the treatment group were relatively similar to the positions in the blank group, indicating that after SKT intervention, the macrophage metabolism of the model mice gradually tended to be normal, and the UC symptoms of mice were relieved by SKT to some extent.

In the energy metabolomics analysis, 10 and 18 differentially expressed metabolites were identified between the treatment group and model group and between the model group and blank group, respectively, and the results are shown in Figure 5c. According to the results of differentially abundant metabolites, KEGG pathway enrichment was performed, and the main metabolic pathways involved were glycolysis and oxidative phosphorylation, as shown in Figure 5d.

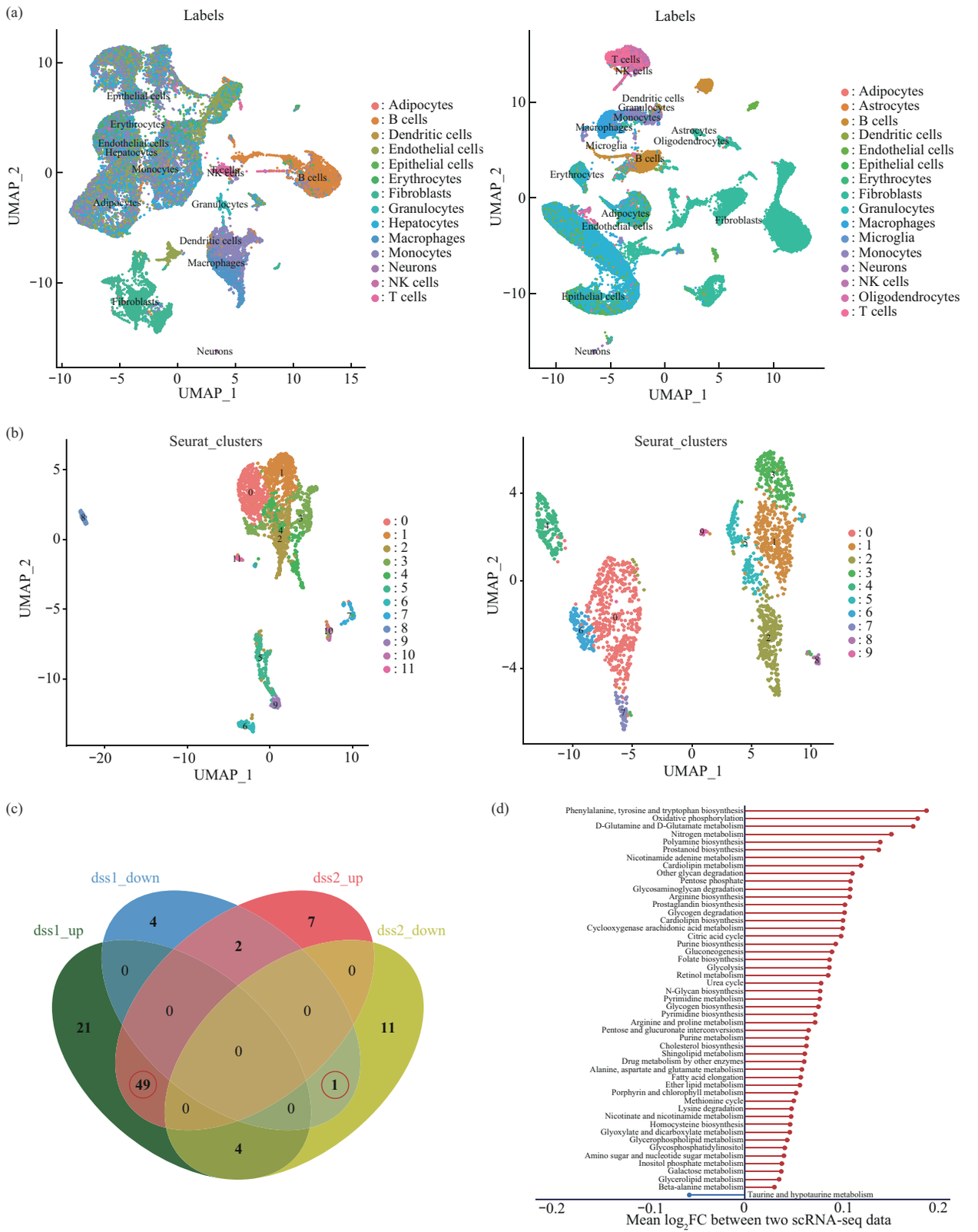

Fig. 4　Single-cell sequencing analysis

(a) Distribution of cell types in the GSE21157 and GSE210415 datasets. (b) Distribution of macrophages in the two groups of data. (c) Distribution of different metabolic pathways of macrophages in the two groups of data. (d) Enrichment of cross difference pathways between two datasets.

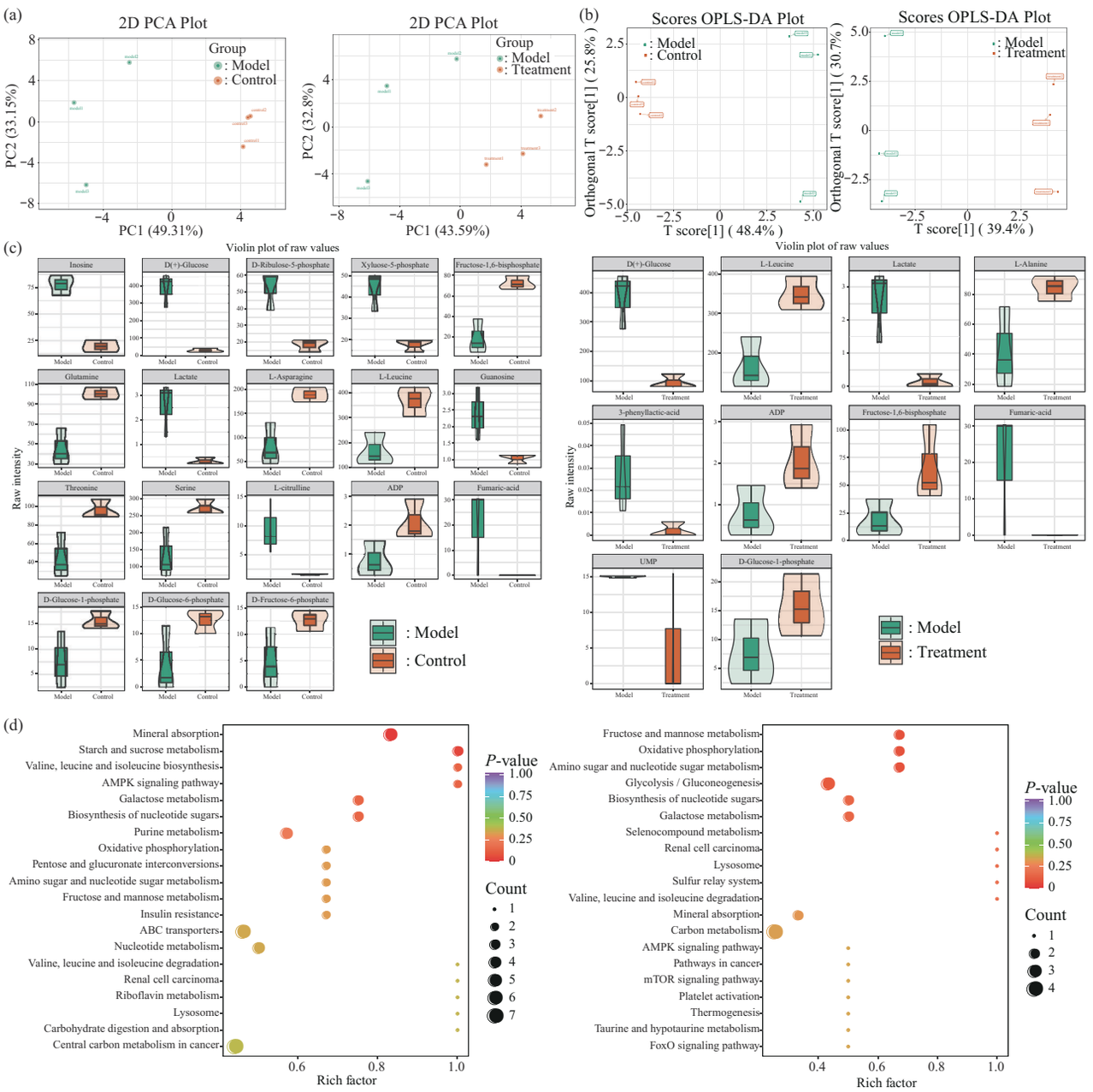

Fig. 5　Energy metabonomic analysis

(a) PCA diagram of macrophage metabolism in mice in each group. (b) OPLS-DA diagram of macrophage metabolism in the blank group and model group. (c) Expression levels of differentially abundant metabolites in mouse macrophages. (d) KEGG enrichment of differentially abundant metabolites. The *x*-coordinate represents the Rich factor corresponding to each pathway, the *y*-coordinate denotes the pathway name, the point color represents the *P* value, and the redder the color, the more significant the enrichment. The point size represents the number of differentially abundant metabolites that were enriched. The screening criteria were *VIP*≥1 and *P*<0.05.

2.5　Test of the causal effect of gene expression on the outcome through multiple Mendelian randomized models

According to the standard IVW SVMR analysis, the predicted genes *HK* (*OR*: 1.87, 95% CI: 1.30−2.15, *P*=0.001 683), *COX4I1* (*OR*: 1.72, 95% CI: 1.57−2.40, *P*=0.003 957), and *TPI* (*OR*: 1.75, 95% CI: 1.58−1.97, *P*=0.030 296) were correlated with the rise of the UC risk, while *NDUFS1* (*OR*: 0.56, 95% CI: 0.48−0.98, *P*=0.000 068) was associated with the reduction of the UC risk. Consistent trends were observed among MR-Egger, weighted median, simple

mode, and weighted mode estimation methods, and the causal effect of gene expression on the outcome was tested through multiple Mendelian randomized models, as shown in Table 2.

Table 2 The causal effect of gene expression on the outcome with multiple Mendelian randomization models

Gene	Method	*OR*	Down 95%CI	Up 95%CI	*P*
HK	MR-Egger	1.907 323	1.332 015	2.205 497	0.978 312
	Weighted median	1.900 642	1.220 095	2.089 101	0.028 577
	Inverse variance weighted	1.870 545	1.298 402	2.149 208	0.001 683
	Simple mode	1.893 711	1.173 859	2.032 125	0.223 599
	Weighted mode	1.901 095	1.314 932	2.296 367	0.135 217
COX4I1	MR-Egger	1.600 236	1.393 289	2.216 076	0.141 611
	Weighted median	1.696 039	1.540 449	2.496 422	0.004 999
	Inverse variance weighted	1.715 627	1.569 965	2.398 516	0.003 957
	Simple mode	1.594 683	1.411 757	2.258 874	0.069 501
	Weighted mode	1.718 886	1.547 383	2.444 123	0.098 194
TPI	Wald ratio	1.753 458	1.583 204	1.973 413	0.030 296
NDUFS1	Inverse variance weighted	0.560 618	0.478 074	0.979 581	0.000 068

2.6 Differentiated mRNA expression of NDUFS1, HK, COX4I1, and TPI in UC datasets

The differences in the transcription levels of NDUFS1, HK, COX4I1, and TPI in the normal colon group and UC group were analyzed by the GSE128682 and GSE102746 datasets, as shown in Figure 6a. Compared with the normal group, the transcription levels of HK1 and HK2 in UC increased, while the transcription level of NDUFS1 in UC declined, and the difference was statistically significant (P<0.05).

2.7 SKT inhibits the polarization of macrophages to the M1 type

The FCM results showed that compared with the control group, the proportion of peritoneal M1 macrophages rose in mice in the DSS group. In comparison with the DSS group, the proportion of M1 macrophages in mice in the DSS+SKT group declined, as shown in Figure 6b. As revealed by the qRT-PCR and Western blot results, the iNOS mRNA and protein expression levels in peritoneal macrophages of mice in the DSS group increased compared with those in the control group. Relative to the DSS group, the iNOS mRNA and protein expression levels of peritoneal macrophages in mice in the DSS+SKT group declined, as shown in Figure 6c.

2.8 SKT promotes the expression level of the oxidative phosphorylation gene NDUFS1

The qRT-PCR and Western blot results reflected that compared with the control group, the NDUFS1 mRNA and protein expression levels in peritoneal macrophages of mice in the DSS group decreased. Compared with those in the DSS group, the NDUFS1 mRNA and protein expression levels in peritoneal macrophages of mice in the DSS+SKT group were increased, as shown in Figure 6d.

2.9 SKT influences the polarization of macrophages toward the M1 type through NDUFS1

Considering the extremely low transfection efficiency of peritoneal macrophages in mice, the RAW264.7 mouse macrophage line was chosen for substitution. A macrophage line with NDUFS1 knocked down was constructed by transfecting sh-NDUFS1 into RAW264.7 cells. According to the qRT-PCR, Western blot, and FCM results, the expression level of iNOS and the proportion of M1 macrophages in the sh-NDUFS1 group increased, and the proportion of M2 macrophages decreased in comparison with the sh-NC group. Compared with the sh-NC+LPS group, the expression level of iNOS and the proportion of M1 macrophages in the sh-NC+LPS+SKT group declined, while the proportion of M2 macrophages increased. No statistically significant differences in the expression level of iNOS and the proportions of M1 and M2 macrophages were observed between the sh-NDUFS1+LPS group and the sh-NDUFS1+LPS+SKT group. In addition, compared with the sh-NC+LPS group/sh-NC+LPS+

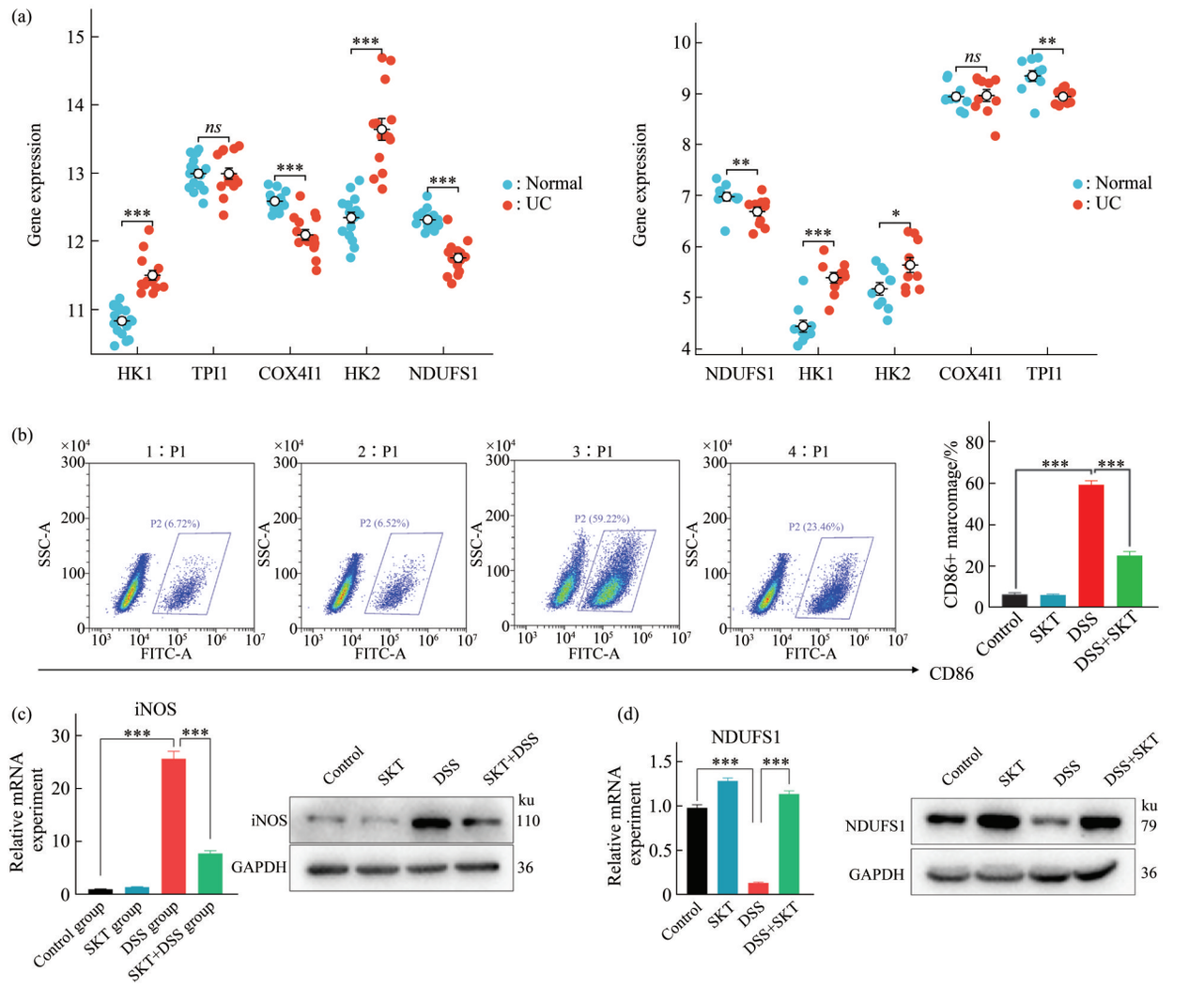

Fig. 6　Detection of iNOS and NDUFS1 protein expression by qRT−PCR and Western blot

(a) Expression difference analysis of NDUFS1, HK, COX4I1, and TPI in the GSE128682 and GSE102746 datasets. (b) Mice were orally administered 3% DSS for 7 consecutive days and treated with 1 g/kg SKT for 14 consecutive days. The peritoneal macrophages of mice in each group were extracted, and the proportion of M1 macrophages was detected *via* FCM. (c, d) Total RNA and protein were extracted from peritoneal macrophages of mice in each group by using TRIzol reagent and RIPA buffer, and the expression levels of iNOS (c) and NDUFS1 (d) in peritoneal macrophages of mice were measured by qRT-PCR and Western blot. GAPDH was used as an internal reference. The data are expressed as the mean± SD (n=3). *ns* no significance, *P<0.05, **P<0.01, ***P<0.001.

SKT group, the expression level of iNOS and the proportions of M1 and M2 macrophages in the sh-NDUFS1+LPS group/sh-NDUFS1+LPS+SKT group decreased. This revealed that knockdown of NDUFS1 promoted the polarization of macrophages to M1 and antagonized the inhibitory effect of SKT on the polarization of macrophages to the M1 type (Figure 7a, c).

To further verify this hypothesis, oe-NDUFS1 was transfected into RAW264.7 cells, and a macrophage line overexpressing NDUFS1 was constructed. qRT-PCR, Western blot, and FCM results showed that compared with the oe-NC group, the expression level of iNOS and the proportion of M1 macrophages in the oe-NDUFS1 group declined, while the proportion of M2 macrophages increased. In comparison with the oe-NC+LPS group/oe-NC+LPS+SKT group, the expression level of iNOS and the proportion of M1 macrophages in the oe-NDUFS1+LPS group/oe-NDUFS1+LPS+SKT group decreased, while the proportion of M2 macrophages was increased. The results revealed that overexpressed

NDUFS1 repressed the polarization of macrophages to the M1 type and strengthened the inhibitory effect of SKT on the polarization of macrophages to the M1 type. In summary, SKT inhibits the polarization of macrophages to the M1 phenotype by promoting the expression of NDUFS1 (Figure 7b, c).

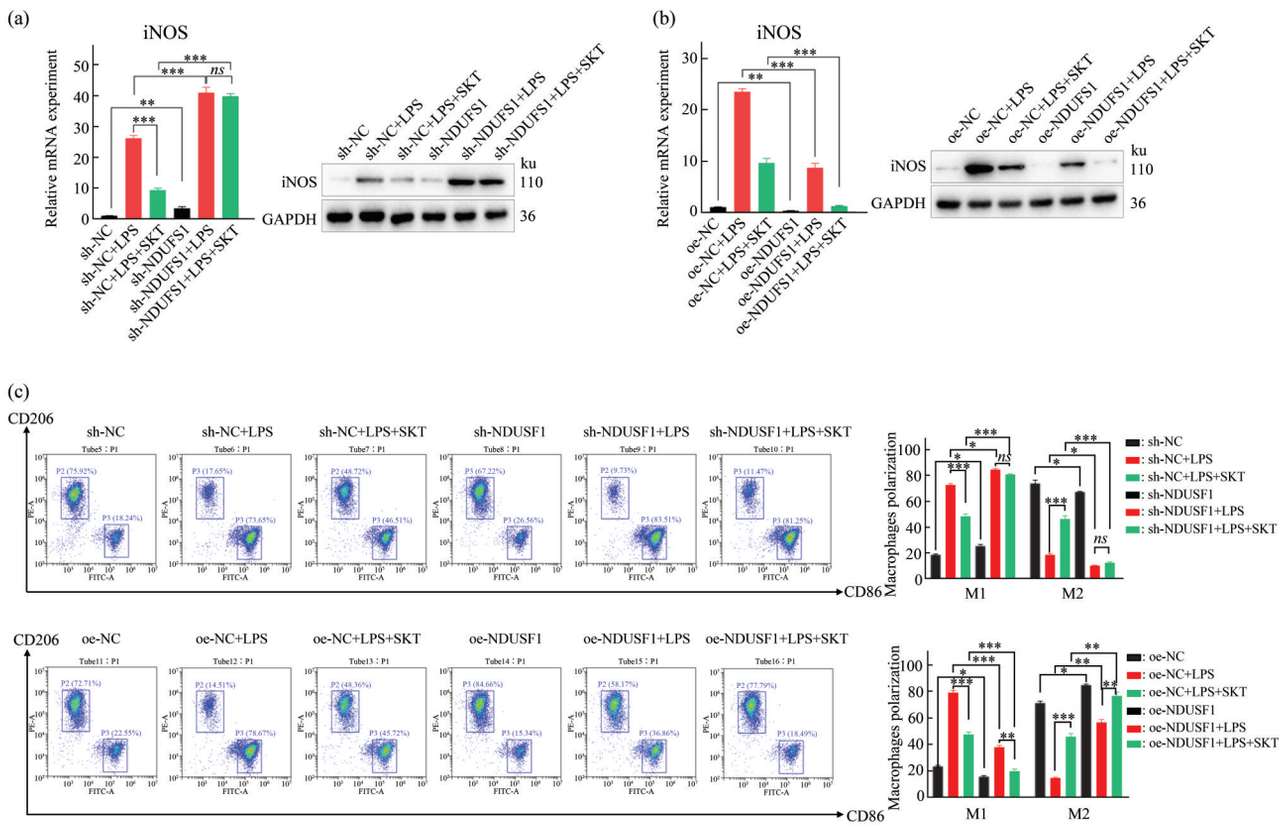

Fig. 7　Effects of sh−NDUFS1 and oe−NDUFS1 transfection on iNOS mRNA and protein expression

(a, b) RAW264.7 cells were transfected with sh-NC and sh-NDUFS1 (a) or oe-NC and oe-NDUFS1 (b) and then incubated with 100 μg/L LPS and 100 μg/L SKT. The total RNA and protein of each group of cells were extracted with TRIzol reagent and RIPA buffer, the expression level of NDUFS1 was then detected *via* qRT-PCR and Western blot, and GAPDH was used as an internal reference. (c) After being transfected with sh-NC and sh-NDUFS1 and oe-NC and oe-NDUFS1, RAW264.7 cells were incubated with 100 μg/L LPS and 100 μg/L SKT, and the proportion of M1 and M2 macrophages was detected through FCM. The data are expressed as the *mean*±*SD* (*n*=3). *ns* no significance, **P*<0.05, ***P*<0.01, ****P*<0.001.

3　Discussion

UC is a chronic inflammatory intestinal disease with complex pathogenesis involving many cell types and signaling pathways. Among them, immune cells, especially macrophages on the intestinal wall, play a key role in the development of UC[13]. Under healthy conditions, the energy of immune cells is mainly generated through the tricarboxylic acid cycle, which, however, is obviously disrupted in UC. The metabolic function of immune cells is regulated by many metabolic pathways, which are significantly changed in UC patients, especially in the case of infection and stress. Single-cell sequencing analysis provides us with a detailed cell composition framework and reveals significant changes in energy metabolic pathways in macrophages in the disease environment of UC. By studying the energy metabolomics of macrophages in UC mouse models, significant differences were observed in metabolites. These differentially abundant metabolites not only involve glycolytic pathways, such as D(+)-glucose and lactate but also involve key metabolites in the tricarboxylic acid cycle, such as fumaric acid. In addition, the study also revealed some metabolic changes related to amino acid metabolism, such as the changes in the levels of L-leucine and L-alanine, which coincide with the reported significant changes in the

concentration of some amino acids in inflammatory bowel diseases[14]. These results suggest that the energy metabolism of intestinal macrophages changes significantly in the disease environment of UC, which may be associated with functional changes in inflammation and tissue repair.

SKT is mainly composed of *Glycyrrhiza uralensis* Fisch. and *Paeonia lactiflor*. In addition, dozens of active components, such as paeoniflorin, gallic acid, catechin, and albiflorin std, were detected by liquid chromatography analysis of SKT extract powder. Paeoniflorin protects mice from DSS-induced colitis by inhibiting inflammation and eosinophil infiltration[15]. Gallic acid also relieves UC symptoms in mice by inhibiting NLRP3 inflammatory corpuscles[16]. Albiflorin std has a positive effect on AMPK-mediated CDX2 expression, which is helpful to alleviate inflammation and cell apoptosis in mouse models[17]. Albiflorin std can reduce inflammation and cell apoptosis in UC mouse models by upregulating AMPK-mediated CDX2 expression[18]. From these preliminary research results, the therapeutic effect of SKT on UC may be related to the comprehensive effect of its various components. These components may work together through various mechanisms, thus alleviating pathological injury to the colon and delaying the progression of UC. The results of this study further support the therapeutic potential of SKT for UC. Specifically, SKT significantly alleviated pathological injury to the colon and delayed the disease progression of UC. In addition, the number of peritoneal M1 macrophages in mice decreased significantly under SKT treatment, meaning that SKT may play a role in regulating the immune response. This is consistent with our observation in the macrophage line *in vitro*, in which SKT obviously inhibits the polarization of macrophages to the M1 type.

Mitochondria, as the most important intracellular energy source, play a core role in cell metabolism, calcium homeostasis, and cell apoptosis. Among them, the oxidative respiratory chain is the key part of mitochondria that performs these functions. As the largest subunit of mitochondrial complex I, NDUFS1 occupies a core position in this chain, regulating electron transfer from NADH to the respiratory chain. As proven by modern medical research, the imbalance of energy homeostasis of colonic mucosa is closely associated with UC. Specifically, the decline in the activity of mitochondrial oxidative phosphorylation is often reflected in the intestinal mucosa of US patients, which may lead to an imbalance in energy metabolism and further aggravate the progression of the disease[19]. Interestingly, the expression of the mitochondrial oxidative phosphorylation complex in intestinal tissues is correlated with age. Respiratory chain complex I increases continuously at the beginning of childhood but decreases gradually in elderly individuals over 60 years old, which may affect cell metabolism, proliferation, and apoptosis[20-21]. According to the Mendelian randomization study, *NDUFS1*, a gene related to oxidative phosphorylation, is associated with the risk reduction of UC. In addition, literature reports reveal that UC is one of the high-risk pathogenic factors of colorectal cancer[22]. It is worth noting that prohibitin 2 (PHB2) promotes the proliferation of colorectal cancer cells and the formation of tumors through NDUFS1-mediated oxidative phosphorylation[23]. It has been pointed out in some studies that electroacupuncture and drug moxibustion can regulate the expression of genes related to oxidative phosphorylation, which, in turn, affects immunity-related pathways such as IgA production and FcγR-mediated phagocytosis in the intestinal immune network, thus alleviating colonic inflammation in rats with DSS-induced UC[24]. In this study, SKT treatment significantly increased the expression of NDUFS1 in peritoneal macrophages, suggesting that SKT may affect the progression of UC by affecting NDUFS1 expression.

Regarding the relationship between UC and mitochondrial function, M1 macrophages play a central role in the disease progression of UC. The activity of aerobic glycolysis and pentose phosphate pathways in M1-type macrophages is enhanced, which leads to the production of inflammatory factors and the activation of the inflammatory response, while M2 macrophages rely more on oxidative phosphorylation to maintain their immunomodulatory function[25]. Studies have shown that triliroside can relieve UC by restoring the balance of M1/M2 macrophages through glycolytic pathways[26]. In this study, it was found through the analysis of GEO datasets that the expression of NDUFS1 in the polarization of macrophages to M1 decreased significantly. *In vitro* experiments showed that when NDUFS1 was knocked down, the M1 polarization of

macrophages was enhanced. Moreover, the M1 polarization of macrophages could be repressed by the overexpression of NDUFS1. This indicates that NDUFS1 may improve UC by inhibiting the M1 polarization of macrophages, and SKT may exert its therapeutic effect by regulating the expression of NDUFS1. Metabolism can regulate the M1/M2 polarization of macrophages and their effects. The polarization and effector function of M1 macrophages depend on the glycolysis of glucose to provide energy. However, the survival and activation of M2 macrophages mainly rely on the oxidation of fatty acids and metabolism in mitochondria, that is, oxidative phosphorylation. The overexpression of NDUFS1 promotes the oxidative phosphorylation of mitochondria, which may further inhibit the transformation of the M1 phenotype and promote the transformation of macrophages to the M2 phenotype. Taking the hallmark gene set in the MsigDB database of GSEA (https://www.The gsea-msigdb.org/gsea/index.jsp) website was used as the reference gene set, and the potential effect pathway of *NDUFS1* in the development of UC was analyzed through the default weighted enrichment statistical method. According to the median expression of NDUFS1, the samples in the sequencing data of colitis patients were subdivided into two groups: the high-expression group and low-expression group, followed by single-gene GSEA. Cibersort, a method commonly used to calculate the infiltration of immune cells, is used to estimate the abundance of immune cells using the deconvolution method for the expression matrix of immune cell subtypes based on the principle of linear support vector regression. To further explore the infiltration degree of M1-type macrophages in UC patients, the infiltration of M1 macrophages in UC patients was analyzed *via* “Cibersort” in R software. The samples in the sequencing data of UC patients were divided into two groups−the high-expression group and low-expression group, according to the media of abundance of infiltrating M1 macrophages, and then GSEA was performed. Next, the signaling pathway entries in the mechanism analysis of NDUFS1 and M1 macrophages were screened out based on the criteria of P<0.05 and NES absolute value≥1. Moreover, the common effect pathways of NDUFS1 and M1 macrophages were drawn *via* the R package “Venn”. A total of 13 common pathways were discovered by taking the intersections of signaling pathways that satisfied the criteria (P<0.05 and NES absolute value≥1), including chemokines, cytokine receptor binding, ECM receptor binding, adhesion plaque, cell adhesion, NOD-like receptor, JAT-STAT, and Toll-like receptor signaling pathways.

Through the analysis of GEO datasets (GSE205990, GSE157182 and GSE76736), it was discovered that compared with unpolarized macrophages, there was no significant difference in the transcription level of HK1 and HK2 in the polarization of macrophages to M1 and M2. Therefore, relevant research on HK1 and HK2 has not been considered to date. Of course, this is only the preliminary bioinformatics analysis result, which will be further probed in a follow-up study. In a literature report[27], the blood-absorbed SKT components that passed the identification of standard substances included albiflorin std, benzoic acid, glycyrrhizic acid, isoliquiritigenin, liquiritin, and paeonol. Molecular docking of such blood-absorbed components with NDUFS1 was investigated. The binding capacity between liquiritin and protein was relatively strong, indicating that liquiritin might be an important material component in SKT that could enhance the expression of NDUFS1 and repress M1 macrophages. SKT contains many compounds that exhibit multitarget effects in the treatment of UC. In this study, the signaling pathway targets correlated with the activity of SKT were verified through bioinformatics and molecular pharmacological experiments. The emphasis was placed on exploring the protective effect of the clinical dose of SKT on UC mouse models and further expounded on its mechanism of action, so no positive controls were set, and no multidose study was implemented.

4 Conclusion

NDUFS1 is potentially related to the polarization of macrophages and the effect of SKT in the treatment of UC. SKT may inhibit the polarization of macrophages to M1 by enhancing the expression of NDUFS1 and ultimately alleviate the progression of UC in mice. This study further deepens the understanding of the pathogenesis and treatment strategy of UC and highlights the value of combining traditional medicine with modern biological research.

References

[1] Glassner K L, Abraham B P, Quigley E M. The microbiome and inflammatory bowel disease. J Allergy Clin Immunol, 2020, **145**(1):16-27

[2] Wu M M, Wang Q M, Huang B Y, *et al*. Dioscin ameliorates murine ulcerative colitis by regulating macrophage polarization. Pharmacol Res, 2021, **172**:105796

[3] Funes S C, Rios M, Escobar V J, *et al*. Implications of macrophage polarization in autoimmunity. Immunology, 2018, **154**(2):186-195

[4] Meselhy R M, Hattori M. Recent studies on peony root and a bioactive constituent, paeoniflorin. Curr Top Phytochem, 2000, **4**: 1-19

[5] Lee K K, Omiya Y, Yuzurihara M, *et al*. Antispasmodic effect of shakuyakukanzoto extract on experimental muscle cramps *in vivo*: role of the active constituents of glycyrrhizae radix. J Ethnopharmacol, 2013, **145**(1): 286-293

[6] Hu S, Luo Y, Yang X, *et al*. Shaoyao gancao decoction protects against dextran sulfate sodium-induced ulcerative colitis by down-regulating ferroptosis. J Pharm Pharmacol, 2023, **75**(8): 1111-1118

[7] 张雪燕, 韩涛, 孟莉 . 芍药甘草汤在溃疡性结肠炎中的应用 . 辽宁中医学院学报, 2004, **6**(4): 280-281
Zhang X Y, Han T, Meng L. J Liaoning Univ Tradit Chin Med, 2004, **6**(4): 280-281

[8] Takeda S, Goto K, Ishige A, *et al*. General pharmacological properties of shakuyaku-kanzo-to. Pharmacometric, 2003, **64**(1): 23-31

[9] Yamamoto K, Hoshiai H, Noda K. Effects of shakuyaku-kanzo-to on muscle pain from combination chemotherapy with paclitaxel and carboplatin. Gynecol Oncol, 2001, **81**(2): 333-334

[10] Zhu N, Hou J, Ma G, *et al*. Network pharmacology identifies the mechanisms of action of shaoyao gancao decoction in the treatment of osteoarthritis. Med Sci Monit, 2019, **25**: 6051-6073

[11] Chang Z P, Deng G F, Shao Y Y, *et al*. Shaoyao-gancao decoction ameliorates the inflammation state in polycystic ovary syndrome rats *via* remodeling gut microbiota and suppressing the TLR4/NF-κB pathway. Front Pharmacol, 2021, **12**: 670054

[12] Chiu Y J, Lin C H, Lee M C, *et al*. Formulated Chinese medicine shaoyao gancao tang reduces NLRP1 and NLRP3 in Alzheimer's disease cell and mouse models for neuroprotection and cognitive improvement. Aging (Albany NY), 2021, **13**(11): 15620-15637

[13] Lai W, Xian C, Chen M, *et al*. Single-cell and bulk transcriptomics reveals M2d macrophages as a potential therapeutic strategy for mucosal healing in ulcerative colitis. Int Immunopharmacol, 2023, **121**: 110509

[14] Balasubramanian K, Kumar S, Singh R R, *et al*. Metabolism of the colonic mucosa in patients with inflammatory bowel diseases: an *in vitro* proton magnetic resonance spectroscopy study. Magn Reson Imaging, 2009, **27**(1): 79-86

[15] Li J J, Ren S Y, Li M, *et al*. Paeoniflorin protects against dextran sulfate sodium (DSS)-induced colitis in mice through inhibition of inflammation and eosinophil infiltration. Int Immunopharmacol, 2021, **97**: 107667

[16] Yu T Y, Feng Y M, Kong W S, *et al*. Gallic acid ameliorates dextran sulfate sodium-induced ulcerative colitis in mice *via* inhibiting NLRP3 inflammasome. Front Pharmacol, 2023, **14**: 1095721

[17] Zheng K, Jia J, Yan S H, *et al*. Paeoniforin ameliorates ulcerative colitis by modulating the dendritic cell-mediated TH17/Treg balance. Infammopharmacology, 2020, **28**(6): 1705-1716

[18] Xu X P, Liu H Y, Pan Y, *et al*. Albiflorin attenuates inflammation and apoptosis by upregulating AMPK-mediated expression of CDX2 in a mouse model of ulcerative colitis. Trop J Pharm Res, 2020, **19**(5): 995-999

[19] Florian B, Wiebke B, Andrea W, *et al*. Mitochondrial gene polymorphisms that protect mice from colitis. Gastroenterology, 2013, **145**(5): 1055-1063

[20] Özsoy M, Zimmermann F A, Feichtinger R G, *et al*. Changes in the expression of oxidative phosphorylation complexes in the aging intestinal mucosa. Exp Gerontol, 2020, **135**: 110924

[21] Stamp C, Whitehall J C, Smith A L M, *et al*. Age-associated mitochondrial complex I deficiency is linked to increased stem cell proliferation rates in the mouse colon. Aging Cell, 2021, **20**(3): e13321

[22] Shi X, Yu J, Lu C, *et al*. Screening of the shared pathogenic genes of ulcerative colitis and colorectal cancer by integrated bioinformatics analysis. J Cell Mol Med, 2023, **28**(5): e17878

[23] Ren L, Meng L, Gao J, *et al*. PHB2 promotes colorectal cancer cell proliferation and tumorigenesis through NDUFS1-mediated oxidative phosphorylation. Cell Death Dis, 2023, **14**(1): 44

[24] Qi Q, Zhong R, Liu Y N, *et al*. Mechanism of electroacupuncture and herb-partitioned moxibustion on ulcerative colitis animal model: a study based on proteomics. World J Gastroenterol, 2022, **28**(28): 3644-3665

[25] Wculek S K, Heras-Murillo I, Mastrangelo A, *et al*. Oxidative phosphorylation selectively orchestrates tissue macrophage homeostasis. Immunity, 2023, **56**(3): 516-530

[26] Zhuang H D, Lv Q, Zhong C, *et al*. Tiliroside ameliorates ulcerative colitis by restoring the M1/M2 macrophage balance *via* the HIF-1α/glycolysis pathway. Front Immunol, 2021, **12**: 649463

[27] Feng L M, Chen Y Y, Xu D Q, *et al*. An integrated strategy for discovering effective components of Shaoyao gancao decoction for treating neuropathic pain by the combination of partial least-squares regression and multi-index comprehensive method. J Ethnopharmacol. 2020, **260**: 113050

芍药甘草汤通过调节NDUFS1表达抑制巨噬细胞向M1极化缓解小鼠溃疡性结肠炎

夏侯志楷[1)] 肖 红[2)] 宋亚锋[1)*] 韩 君[3)*]

([1)] 北京体育大学中国运动与健康研究院，北京 100084；

[2)] 北京体育大学运动人体科学学院，北京 100084；[3)] 北京康仁堂药业有限公司中药研究院，北京 101301）

摘要 目的 本研究旨在探索并阐明芍药甘草汤（Shakuyakukanzoto，SKT）通过调节巨噬细胞的能量代谢和极化来改善小鼠溃疡性结肠炎（ulcerative colitis，UC）的可能作用机制。**方法** 通过给予3%葡聚糖硫酸钠盐（dextran sulfate sodium salt，DSS）构建小鼠UC模型并通过灌胃SKT进行治疗。首先，对两个数据集GSE21157和GSE210415进行单细胞测序分析和代谢通路富集。其次，对UC小鼠腹腔巨噬细胞的提取和代谢组学验证。然后，根据标准逆方差加权两样本的单变量孟德尔随机化分析差异代谢物富集的通路和UC风险相关性。接着，分析在GSE128682和GSE102746数据集转录水平差异。最后，使用定量反转录PCR（qRT-PCR）、蛋白质印迹法（Western blot）和流式细胞术验证结果。**结果** 苏木精-伊红（HE）染色结果显示，SKT可以显著缓解DSS引起的结肠损伤。单细胞测序分析在肠壁中发现了巨噬细胞、NK细胞、T细胞等10多种不同类型的细胞。在疾病组中，通过比较这两组数据发现，有49条主要涉及能量代谢的巨噬细胞代谢途径的活性显著上调。能量代谢组学中，治疗组与模型组，模型组与空白组分别鉴定了10种和18种显著上调和下调的差异表达代谢物，这些差异表达的代谢物主要与糖酵解和氧化磷酸化有关。根据标准逆方差加权两样本的单变量孟德尔随机化分析，预测糖酵解和氧化磷酸化相关基因泛醌NADH脱氢酶Fe-S蛋白1（recombinant NADH dehydrogenase ubiquinone Fe-S protein 1，*NDUFS1*）（*OR*：0.56，95% CI：0.48~0.98，*P*=0.000 068）与UC风险降低相关。通过对两组数据集转录水平差异分析，与正常组相比，UC中NDUFS1的转录水平降低。qRT-PCR、Western blot和流式细胞术验证结果显示，SKT可以促进NDUFS1蛋白的表达，抑制巨噬细胞向M1型极化。此外，敲低/过表达NDUFS1可以影响SKT对巨噬细胞M1型极化的影响。**结论** SKT通过调节NDUFS1蛋白水平，抑制巨噬细胞向M1型极化，从而缓解小鼠UC。这些发现不仅揭示了SKT对UC的治疗机制，也为临床应用提供了新的理论基础。

关键词 芍药甘草汤，巨噬细胞M1型极化，氧化磷酸化，溃疡性结肠炎

中图分类号 R574，R932 **DOI**：10.16476/j.pibb.2023.0347

* 通讯联系人。

宋亚锋 Tel：010-62962180，E-mail：songyafeng@bsu.edu.cn

韩君 Tel：18311059115，E-mail：729229056@qq.com

收稿日期：2023-09-02，接受日期：2023-10-26